European Journal of Immunology

Acute cytomegalovirus infection modulates the intestinal microbiota and targets intestinal epithelial cells

Vu Thuy Khanh Le-Trilling[a*#], Jana-Fabienne Ebel[b*], Franziska Baier[b], Kerstin Wohlgemuth[a], Kai Robin Pfeifer[b], Aart Mookhoek[c], Philippe Krebs[c], Madita Determann[a], Benjamin Katschinski[a], Alexandra Adamczyk[b], Erik Lange[b], Robert Klopfleisch[d], Christian M. Lange[e], Viktoriya Sokolova[b,f], Mirko Trilling[a] & Astrid M. Westendorf[b#]

[a] *Institute for Virology, University Hospital Essen, University of Duisburg-Essen, Essen, Germany*
[b] *Institute of Medical Microbiology, University Hospital Essen, University of Duisburg-Essen, Essen, Germany*
[c] *Institute of Pathology, University of Bern, Bern, Switzerland.*
[d] *Institute of Veterinary Pathology, Free University of Berlin, Berlin, Germany*
[e] *Department of Gastroenterology and Hepatology, University Hospital Essen, University of Duisburg-Essen, Essen, Germany*
[f] *Inorganic Chemistry and Centre for Nanointegration Duisburg-Essen (CeNIDE), University of Duisburg-Essen, Essen, Germany*
* *contributed equally*
[#] **Corresponding authors:**

Astrid M. Westendorf, Infection Immunology, Institute of Medical Microbiology, University Hospital Essen, Hufelandstr. 55, 45122 Essen, Germany. E-mail: astrid.westendorf@uk-essen.de (lead contact)

Vu Thuy Khanh Le-Trilling, Institute for Virology University, Hospital Essen, Hufelandstr. 55, 45122 Essen, Germany. E-mail: Khanh.Le@uk-essen.de

Abstract

Primary and recurrent cytomegalovirus (CMV) infections frequently cause CMV colitis in immunocompromised as well as inflammatory bowel disease (IBD) patients. Additionally, colitis occasionally occurs upon primary CMV infection in patients who are apparently immunocompetent. In both cases, the underlying pathophysiologic mechanisms are largely elusive - in part due to the lack of adequate access to specimens. We employed the mouse cytomegalovirus (MCMV) model to assess the association between CMV and colitis. During acute primary MCMV infection of immunocompetent mice, the gut microbial composition

Received: 12/04/2022; Revised: 14/10/2022; Accepted: 14/10/2022

This article has been accepted for publication and undergone full peer review but has not been through the copyediting, typesetting, pagination and proofreading process, which may lead to differences between this version and the Version of Record. Please cite this article as doi: 10.1002/eji.202249940.

was affected as manifested by an altered ratio of the *Firmicutes* to *Bacteroidetes* phyla. Interestingly, these microbial changes coincited with high-titer MCMV replication in the colon, crypt hyperplasia, increased colonic pro-inflammatory cytokine levels, and a transient increase in the expression of the antimicrobial protein Regenerating islet-derived protein 3 gamma (Reg3γ). Further analyses revealed that murine and human intestinal epithelial cell lines, as well as primary intestinal crypt cells and organoids represent direct targets of CMV infection causing increased cell death. Accordingly, *in vivo* MCMV infection disrupted the intestinal epithelial barrier and increased apoptosis of intestinal epithelial cells. In summary, our data show that CMV transiently induces colitis in immunocompetent hosts by altering the intestinal homeostasis.

Keywords: cytomegalovirus, colitis, microbiota, intestinal organoids, epithelial cells

Introduction

Cytomegaloviruses (CMVs) are prototypical members of β-herpesvirinae. The majority of the global adult population is latently infected with human CMV (HCMV). Although most HCMV infections in immunocompetent adults progress subclinically, fatal infections sporadically occur in apparently healthy individuals [1]. CMV colitis emerges most commonly in immunocompromised hosts due to primary infections or reactivation events of latent CMV. However, CMV colitis can also occur in healthy patients without immunodeficiency – usually in a setting of primary infection [2, 3]. The typical clinical presentation of CMV colitis includes abdominal pain, fatigue, fever, non-bloody or bloody diarrhea, and weight loss. Intriguingly, all these symptoms overlap with the clinical presentation of inflammatory bowel disease (IBD) [4, 5]. IBD constitutes a group of intestinal disorders that cause chronic inflammation of the digestive tract. The precise etiology of IBD is unknown. The prevailing hypothesis suggests that IBD results from an exaggerated immune response that is triggered by environmental factors towards altered gut microbiota or

pathogenic microorganisms in a genetically prone host [6-8]. Interestingly, the prevalence of active CMV infection in the colon is considerably higher in patients with IBD compared to control populations [9] and CMV infections are associated with more severe manifestations of IBD [10, 11].

The gut microbiome exhibits many critical roles in maintaining human health [12] and is involved in the development and maintenance of the host immune system [13]. It is generally accepted that IBD is associated with microbial alterations; however, it is unclear whether such alterations cause intestinal inflammation or rather represent a consequence of it. Alterations of the gut flora are also well documented in different viral infections [14, 15]. In human immunodeficiency virus (HIV) and simian immunodeficiency virus (SIV) infections, correlations between microbial dysbiosis and inflammatory cytokine production in the gut were observed and, importantly, linked to chronic immune activation [16]. For persistent CMV infections, alterations in the microbiota have been also reported. Santos Rocha *et al*. [17] found that RhCMV infections of rhesus macaques are associated with a significantly altered composition of gut microbiota and increased host immune cell activation. However, it remained unclear whether this is a long-term consequence of the conditions induced by persistent infection or whether an acute CMV infection may be sufficient to trigger alterations in the gut microbiota and thereby influence the host immunity.

In the present study, we provide evidence that acute primary MCMV infection of immunocompetent mice alters the gut microbial composition and is accompanied by high-titer virus replication in the colon, mild pathological changes in gut architecture, higher levels of colonic pro-inflammatory cytokines, and a leaky intestinal epithelial barrier. These *in vivo* findings were corroborated by studies employing murine and human primary intestinal epithelial cells in complex organoids, indicating that epithelial cells exhibit high rates of cell mortality upon CMV infection. Furthermore, immunohistochemistry of colonic tissue

sections from IBD patients with a concurrent CMV replication showed that HCMV infects, among others, intestinal epithelial cells. Our findings suggest a pathomechanism by which CMV infections may interfere with intestinal homeostasis and foster inflammation in the gastrointestinal tract.

Results:

MCMV infection alters the microbial composition in the feces.

While the modulation of the commensal microbiota by viruses has been described in the literature, there is a lack of information regarding the effect of primary CMV infection on gut microbiota and the association with host immunity. To investigate the consequences of an acute primary CMV infection on the microbial composition in an immunocompetent host, we collected feces samples of mice before infection and at day 2 and 5 post-infection. If not stated otherwise, BALB/c mice were infected with cell culture-derived MCMV by intraperitoneal injection. From the feces, DNA was extracted and the V3-V4 regions of the 16S rRNA gene were sequenced. A total of 5 bacterial phyla were detected in all analyzed samples. The predominant phyla were *Firmicutes* and *Bacteroidetes*, followed by *Proteobacteria*, *Deferribacterota* and *Actinobacteria*, which were less abundant (Figure 1 A). No significant differences in the relative abundance of *Proteobacteria*, *Deferribacterota*, and *Actinobacteria* were observed between fecal samples from mice before infection ('non-infected') and from the same mice 2 and 5 days post MCMV infection. In contrast, at 2 and 5 days post MCMV infection, the abundance of the phylum *Firmicutes* was decreased and the phylum *Bacteroidetes* was substantially more abundant (Figure 1 A). The ratio of *Firmicutes to Bacteroidetes* has been used to express the degree of dysbiosis in the colon [18]. Of note, this ratio was reduced in infected mice, regardless of the days post-infection (Figure 1 B). When we determined whether the microbial changes in the phyla are based on alterations on family level, no changes in one specific family was detected in the *Firmicutes* phylum, rather,

we observed a slight decrease in all families (data not shown). In contrast, there were higher abundances of *Rikenellaceae* and *Prevotellaceae* families in the *Bacteroidetes* phylum at day 5 post-infection compared to the mice before infection (Figure 1 C). To analyze if the observed CMV-driven dysbiosis is a long-lasting or rather a short-term effect, we infected BALB/c mice with MCMV, and collected feces samples before infection and at day 2, 7, 10, and 12 post-infection. DNA was extracted and relative abundance of the phyla *Firmicutes* and *Bacteroidetes* was analyzed via quantitative PCR. In accordance with aforementioned results, the ratio of *Firmicutes* to *Bacteroidetes* was reduced early post-infection, but this effect was completely receded at day 7 to 12 post-infection (Figure 1D), suggesting gut dysbiosis as an early transient event in MCMV infection.

MCMV infection induces mild colonic inflammation with secretion of pro-inflammatory cytokines.

A reduced ratio of *Firmicutes* to *Bacteroidetes* and an enhanced abundance of *Rikenellaceae* and *Prevotellaceae* are associated with intestinal inflammation in patients suffering from IBD [18-20]. To evaluate potential direct effects of MCMV on the gut homeostasis, we first determined viral loads in different organs at day 5 post-infection. As expected from previous work [21], we observed high viral titers in the spleen, liver, and salivary glands of MCMV-infected animals. Given that the intestinal organs are not routinely assessed by most MCMV researchers, we were surprised to find that MCMV replication in the colon reached virus titers that were comparable to the amounts of virus in livers and spleens. In these different organs, MCMV titers of approximately 10^3 - 10^5 PFU per gram of tissue were found (Figure 2 A).

To better understand the effects of MCMV on the gut, we determined the colonic viral loads in a longitudinal manner and compared the results to the viral loads in spleen, liver, and salivary glands (Figure 2 B). As expected, very high viral titers in the spleen and liver were

detected early at day 2 and 5 post-infection with a very strong decline at day 7. Intriguingly, the colon showed a specific kinetic of virus replication. In contrast to spleen and liver, viral replication in the colon was delayed, starting at 2 days post-infection, peaking at day 5, and still profound viral titers were observed at 7 days post-infection. As expected, viral titers in the salivary glands started to increase at 5 days post-infection and further increased at later time points.

Intrigued by the MCMV replication in the colon, we analyzed whether the high colonic MCMV titers were associated with changes in the colonic architecture. For this purpose, we infected BALB/c mice with MCMV and performed histological analysis of the colon at the time point with the highest virus load (day 5 post-infection). Interestingly, mild crypt necrosis and an enhanced epithelial hyperplasia, indicated by a significant increase in the crypt length 5 days post infection, were observed in MCMV-infected animals (Figure 3 A). These changes in the colonic architecture were associated with stronger colonic secretion of TNF-α, IFN-γ, and in tendency enhanced IL-6 levels (Figure 3 B).

Since we observed that MCMV infection (i.p.) of BALB/c mice disturbs the gut homeostasis, we analyzed which host cell-derived factors may induce the changes in the microbial composition. To this end, the expression of antimicrobial molecules in the gut was measured longitudinally. We observed a transient increase in Reg3γ expression shortly after MCMV infection at day 1 and 2 post infection followed by a later return to baseline levels (Figure 3 C). These data raised the question whether the change in the gut microbial composition is a cause of colonic inflammation or a consequence of MCMV-induced intestinal inflammation. To address this, we treated BALB/c mice daily with a cocktail of antibiotics (Abx) by oral gavage starting 4 days before MCMV infection and during the course of infection. First, we determined MCMV titers in Abx-treated vs. non-treated mice. Of note, no difference in virus titers were observed in spleen, liver, and colon between Abx-treated and non-treated animals

(Figure 4 A). Next, we assessed if the presence of the microbiota interferes with CMV-induced crypt hyperplasia. Interestingly, we observed a slight increase in the crypt length due to Abx treatment, but no further enhancement was induced after MCMV infection (Figure 4 B). In accordance, the secretion of colonic TNF-α and IFN-γ was slightly reduced in MCMV-infected animals with Abx treatment compared to MCMV infection without Abx treatment but no difference in IL-6 secretion was observed (Figure 4 C). The data obtained for Reg3γ expression and the results from the Abx treated-animals suggest that the changes in the microbial composition are more the cause than the consequence of inflammation in our experimental setting.

MCMV infection disturbs the intestinal barrier integrity.

Since MCMV is a cytolytic virus and IFN-γ and IL-6 can modulate the intestinal barrier [22, 23], we tested whether MCMV infection (i.p.) affects the intestinal permeability *in vivo*. Naive and 5 day MCMV-infected BALB/c mice were orally gavaged with FITC-labeled dextran beads. Four hours later, the intestinal permeability was assessed by determination of FITC-dextran beads translocated from the gut lumen to the blood stream. In accordance with the finding that the cytolytic MCMV replicates in intestinal tissues and alters their morphology, FITC-dextran concentrations in the serum of MCMV-infected mice were significantly increased compared to naive control mice (Figure 5 A). In addition, the level of apoptosis in the colonic epithelium was determined by immunostaining of cleaved caspase-3. As shown in Figure 5 B, colon tissue sections of MCMV-infected mice exhibited a significant increase in caspase 3 positive epithelial cells. To check if epithelial cells can be a direct target of MCMV infection, we infected BALB/ mice with MCMV expressing GFP and performed immunohistochemistry staining for GFP in colonic sections. Consistent with our hypothesis, we observed the presence of MCMV-GFP-positive intestinal epithelial cells (Figure 5 C). These data provide clear evidence that MCMV infection affects the intestinal

epithelium, causing a mild inflammation and an impairment of intestinal barrier functions in immunocompetent hosts.

Murine intestinal epithelial cell lines and organoids are highly susceptible to MCMV infection.

To define the role of intestinal epithelial cells during gastrointestinal infection, we further investigated the susceptibility of these cells to CMV infection using a murine intestinal epithelial cell line (MODE-K) and primary intestinal organoids. First, MODE-K cells were mock-treated or infected with MCMV expressing GFP at graded virus doses (0.007 - 10 PFU/cell). As infection control, we used highly MCMV-permissive immortalized mouse embryonic fibroblasts (iMEF; described in [24]). Interestingly, MODE-K cells were nearly as susceptible to MCMV infection as the highly permissive iMEFs, as indicated by the GFP signal intensity 24 h post-infection in higher dilutions of the input virus (Figure 6 A). This was verified by the quantification of plaque-forming units from the supernatant of infected MODE-K and iMEF cells (Figure 6 B) and the visualization of plaque formation (Figure 6 C).

To bridge the gap regarding the cellular complexity between simple 2D cell cultures and complex *in vivo* infections, we set up a protocol for the MCMV infection of intestinal organoids. Intestinal organoids are derived from self-organizing and self-renewing intestinal stem cells and closely recapitulate the native intestinal epithelium. This *ex vivo* model for the gut fully reproduces the structural architecture of the intestinal epithelium and contains all major intestinal cell lineages [25, 26]. Intestinal organoids were established by isolating intestinal crypts containing stem cells from the gut of BALB/c mice and culture for 5-10 days until the development of differentiated organoids (Figure 6 D, Mock). Differentiated intestinal organoids were harvested and infected with MCMV-GFP at an MOI of 1 and 10. At day 2 post-infection, we identified infected cells by immunofluorescence microscopy (Figure

6 D). Different spots of infection were detected within the intestinal organoids with an enlargement of the infected host cells. To enable a visualization of epithelial cells within organoids and to infallibly ensure their intestinal origin as well as the epithelial identity, we isolated intestinal crypts from ROSA26/LSL-tdTom x Villin-Cre (Vil-tomato) mice that specifically express the red fluorescent protein tdTomato in intestinal epithelial cells (Figure 6 E). Again, differentiated intestinal organoids were harvested and infected with MCMV-GFP. At day 3 post-infection, we identified infected GFP-positive cells within the red epithelial cell layer by immunofluorescence microscopy (Figure 6 E). Taken together, our data showed that murine primary intestinal epithelial cells as single cells and in complex organoids are permissive for CMV infection.

Survival of intestinal organoids is affected by MCMV infection.

In multicellular organisms, regulated cell death programs are essential for the elimination of damaged, transformed or unwanted cells. In addition, cell death has the capacity to act as defense mechanism against invading pathogens - especially in the case of intracellular pathogens [27]. Consequently, CMVs encode multiple death inhibitors that are required for efficient viral replication [28]. To investigate how intestinal organoids react to MCMV infection in terms of organoid morphology and survival, we isolated intestinal crypts and differentiated intestinal organoids for 7 days, and infected them with increasing doses of MCMV. As control, we treated organoids with UV-inactivated MCMV at a calculated MOI of 10. In the mock-treated group, 80% of the organoids were intact and showed typical crypt formation (‘budding’) at day 6 post-infection (Figure 7 A). In contrast, with increasing virus dose, the organoids started to die, resulting in a substantial decrease in the proportion of crypt-forming organoids (Figure 7 A and B). Of note, treatment with UV-inactivated MCMV did not significantly alter the organoid morphology or induced cell death (Figure 7 A). Thus, MCMV is not able to prevent the cell death of infected intestinal organoids.

To determine the consequences of MCMV-associated crypt necrosis and the survival of crypt stem cells *in vivo*, we isolated colonic crypts from non-infected and MCMV-infected BALB/c mice and plated these for the formation of organoids. The absolute number of colonic crypts was significantly lower when isolated from MCMV-infected mice compared with non-infected mice (Figure 8 A). The enteroid forming efficiency was determined by counting the exact number of crypts per well after plating and the number of intact organoids formed from the crypts after 24 h. Importantly, the enteroid forming efficiency was significantly reduced after MCMV infection (Figure 8 B), but the overall survival and morphology of finally formed organoids was not altered (Figure 8 C/D). Altogether, these results suggest that MCMV infection directly affects the survival of crypt stem cells *in vivo*.

Human intestinal epithelial cell lines and organoids are highly susceptible to HCMV infection.

To address the general relevance of our findings from murine studies, we assessed whether primary human intestinal epithelial cells are permissive for HCMV infection by using human gut-derived organoids. Upon full differentiation, organoids were infected with HCMV expressing GFP and at 3 days post HCMV exposure, infection was analyzed by immunofluorescence microscopy. Similar to the results with murine organoids, different spots of infection were detected within the intestinal organoid with an enlargement of the infected host cells and first signs of cell death (Figure 9 A).

Next, we performed immunohistochemistry staining for HCMV in colonic sections to determine the colonic target cells for CMV. To increase the number of colonic spots of infection, we used sections from IBD patients with a concurrent HCMV replication. Consistent with our *in vitro* studies, we observed, although in rare cases, the presence of HCMV-positive intestinal epithelial cells (Figure 9 B). In summary, our findings indicate that

murine and human primary intestinal epithelial cells are permissive for CMV entry and gene expression with an increased cell mortality upon CMV infection.

Discussion

CMV infections are usually controlled and confined by the adult immune system of the healthy host. However, CMV can invade end organs and can cause tissue-invasive diseases such as colitis, gastritis, or enteritis [29]. CMV diseases mainly occur in immunocompromised patients, but cases have also been reported in apparently immunocompetent patients, especially after primary CMV infection [2, 3]. The gastrointestinal mucosa is a major site of opportunistic CMV replication, causing or exacerbating intestinal inflammation that may result in severe end-organ dysfunction [30, 31]. Although the clinical manifestations of intestinal CMV infections are well described, the pathophysiologic mechanisms by which CMV promotes intestinal inflammation and the role of the microbiome in this process remain poorly understood. Especially in light of the clinical relevance of CMV colitis, it is surprising that MCMV replication in the intestine has been largely neglected. Accordingly, the gastrointestinal tract is not mentioned as a potential organ for MCMV replication in the standard reference protocol collection for MCMV *in vivo* analyses [32]. Contamination problems that may arise in cell culture caused by the gut microbiome may be one reason for this.

Even though the relative contribution may vary among different viruses, the influence of the microbiota on the susceptibility to viral infections and the outcome of infectious diseases is undisputable. Santos Rocha *et al*. [17] analyzed the microbiota of RhCMV-infected rhesus macaques. Interestingly, they identified significantly altered gut microbiota and increased host immune cell activation in subclinically infected animals. However, they could not differentiate whether this is a long-term effect of persistent infection or due to an acute CMV infection. Here, we showed that an acute primary CMV infection of immunocompetent mice

is sufficient to induce alterations in the microbial composition. In more detail, the relative abundance of the phylum *Firmicutes* was reduced and the abundance of bacteria belonging to the phylum *Bacteroidetes* was enhanced. The fecal ratio of *Firmicutes* to *Bacteroidetes* has been used as proxy for the health status of a host [33]. Interestingly, we found that the ratio of *Firmicutes* to *Bacteroidetes* was significantly reduced during acute CMV infection at day 2 and 5 post-infection but completely resolved from day 7 post-infection. Recent evidence indicates that such changes in the ratio are associated with the appearance of a number of inflammatory disorders and systemic diseases including gastrointestinal diseases such as IBD [18-20, 34]. Thus, acute primary CMV infection may temporarily alter the microbial community towards a composition that fosters intestinal inflammations. In line with this hypothesis, we identified early upregulation of antimicrobial Reg3γ and high viral titers in the colon of MCMV-infected immunocompetent mice, associated with mild crypt necrosis and significantly enhanced hyperplasia of the intestinal epithelial cells during acute primary MCMV infection. This is further supported by the fact that a reduction of the microbial community by Abx treatment before infection decreased crypt hyperplasia and TNF-α levels.

CMV infection is of particular interest with regard to IBD as the prevalence of active CMV infection in the colon is considerably higher in patients with IBD relative to control patients [9] and CMV infection seems to be associated with more severe IBD [10]. Similarly, we observed HCMV-positive intestinal epithelial cells in an IBD patient associated with HCMV, but the existence of a correlation/association does not necessarily indicate causality. Nevertheless, CMV infection experiments in mouse models of IBD have shown that acute and latent CMV infection exacerbates intestinal inflammation [35-38]. Although the underlying mechanism are not entirely understood, it was demonstrated that concomitant MCMV infection increased gross bleeding [35], induced the production of pro-inflammatory

cytokines or chemokine ligands in the colon [36, 38], or stimulated gut immune responses to the gut microbiota [37].

It is still of debate which cells in the colon are targeted by CMV infection. Replication of the virus in endothelial cells could generate vasculitis associated with microvessel thrombosis and local ulceration [39, 40]. Furthermore, the recruitment of CMV-infected monocytes to the mucosa that promotes the dissemination of inflammatory macrophages in the inflamed tissue was reported [41, 42]. We detected mild colonic crypt necrosis and a significant increase in apoptotic epithelial cells in MCMV-infected immunocompetent mice suggesting epithelial cells as a target for CMV. Necrosis is a passive but uncontrolled process, initiated by external factors such as viral infections and is characterized by a rapid breakdown of the cell membrane, resulting in the release of intracellular compounds into the extracellular space with concomitant activation of the immune system [43]. Accordingly, we measured elevated levels of colonic TNF-α, IFN-γ, and IL-6 in MCMV-infected mice. To define the role of intestinal epithelial cells during gastrointestinal infection in more detail, we made use of primary intestinal organoids. Interestingly, primary murine and human organoids are permissive for CMV infection. CMV is known to encode multiple death inhibitors that are required for efficient viral replication [28]. Nevertheless, CMV was not able to prevent the cell death of infected intestinal organoids in our experimental setup. Maidji *et al.* [44] developed a SCID-hu gut mouse model where the authors subcutaneously implanted human fetal gut into immune-deficient SCID mice. This fetal intestine developed into a differentiated human intestine with a lumen and morphologically precise mucosal layers within 4 weeks. At this stage, the authors intraluminally inoculated the human gut with CMV. Interestingly, they observed substantial CMV infection with marked mucosal damage after 7 days and a rapid depletion of epithelial cells from the fetal intestine differentiated *in vivo*.

Accordingly, we could show a reduction in the *in vitro* enteroid forming efficiency in MCMV-infected immunocompetent animals compared to non-infected animals.

Profound cell death like apoptosis or necroptosis of intestinal epithelial cells interferes with the integrity of the intestinal barrier [45]. In accordance, significantly more apoptotic epithelial cells were detected in the colon of MCMV-infected mice. Furthermore, IL-6 and IFN-γ, which are secreted in the colon during MCMV infection, were described to decrease the intestinal barrier [22, 23]. Consequently, it was shown that CMV infection disrupts the tight junctions of polarized epithelial cells and the adherent junctions of polarized endothelial cells *in vitro* [44]. We could now demonstrate that MCMV infection of immunocompetent mice affects intestinal epithelial cells and significantly enhances the intestinal permeability *in vivo*, thus favoring the translocation of commensals and antigens from the lumen to the *lamina propria,* thereby boosting intestinal inflammation. In summary, our results suggest that primary infection with CMV modulates the intestinal microbiota and mucosal integrity and, consequently, alters the risk for intestinal inflammation and may predispose to the development of IBD. In addition, the surprisingly efficient MCMV replication in the gut and the intestine-specific replication kinetics raises numerous intriguing future questions, e.g., regarding tissue-specific immune responses as well as viral adaptations to this special niche.

Materials and Methods

Human colon biopsies. Colonic biopsies were provided from two healthy donors. Informed consent was obtained from all donors. Stained tissue sections from IBD patients with CMV association were provided by the Tissue Bank Bern (Switzerland), and images were selected among 20 anonymized cases.

Mice. All mice were 8 to 15 weeks old, bred and housed in accordance to the guidelines of the Laboratory Animal Facility of the University Hospital Essen. BALB/c were obtained

from Envigo RMS GmbH. ROSA26/LSL-tdTom were obtained from the Jackson Laboratory and crossed to Villin-Cre mice [46].

Cells, viruses, virus titration and antibiotic treatment. Primary mouse fibroblasts (mouse embryonic fibroblasts [MEF] and mouse newborn cells [MNC]) were isolated from mouse embryos and newborns, respectively, according to described protocols [47]. Mouse fibroblasts were grown in Dulbecco`s minimal essential medium (DMEM) supplemented with 10% (v/v) FCS, 100 µg/ml streptomycin, 100 U/ml penicillin, and 2 mM glutamine. Murine MODE-K [48] cells were cultivated in Roswell Park Memorial Institute (RPMI)-1640 supplemented with 10% (v/v) FCS, 100 µg/ml streptomycin, 100 U/ml penicillin, and 2 mM glutamine. All cell culture media and supplements were obtained from Gibco (Life technologies, Darmstadt, Germany). The wt-MCMV was reconstituted from the MCMV-BAC described in Jordan *et al.* [49]. MCMV-GFP has been previously described [50, 51]. MCMV propagation and determination of viral titers by standard plaque titration were performed using primary MEF or MNC [47]. All *in vitro* infections and titrations were conducted with centrifugal enhancement (900 g for 30 min). For *in vivo* infections, mice were infected intraperitoneally with $2*10^5$ PFU MCMV per mouse. Organs of infected mice were harvested, snap frozen in liquid nitrogen, and stored at -80°C until titrations were performed. For microbiota depletion, mice were orally gavaged with 1 mg vancomycin, 2 mg metronidazole, 2 mg ampicilin and 2 mg neomycin dissolved in drinking water. Mice were treated daily starting 4 days prior infection and for the duration of infection. Control groups received drinking water following the same protocol. HCMV-GFP (TB40EΔgpt EGFP [52]) was propagated as described in Le-Trilling *et al.* [53]. Viral GFP reporter gene expression was quantified by use of a microplate multireader (Mithras LB 943; Berthold Technologies GmbH & Co.KG, Bad Wildbad, Germany).Viral plaque formation was visualized by

infection with GFP-expressing CMV followed by image acquisition with a Leica THUNDER imager.

DNA extraction and sequencing. Feces samples were collected and stored at -80°C. DNA was extracted using Zymo Biomics DNA miniprep kit (Zymo, Freiburg, Germany). Genomic DNA was used for qPCR analysis [54] or prepared for sequencing following the protocol #15044223 Rev. B provided by Illumina technical support: Regions V3 and V4 of the 16S rRNA gene were amplified, and samples were labelled with index primers using Nextera XT Index kit (Illumina, San Diego, CA, USA). Paired end sequencing was performed with the Illumina MiSeq system. Sequenced raw data was re-multiplexed employing the Perl programing language. By utilizing the Integrated Microbial Next Generation Sequencing [55] platform, reads with a similarity of at least 97% were assigned to operational taxonomic units (OTUs). OTU-based microbial profiles were built as described by Lagkouvardos *et al.* [56]. The OTU-based profiles where examined regarding sequencing depth, alpha diversity, relative abundances of different OTUs assigned to taxonomic levels within each sample, beta diversity, and diversity between different groups of samples. Also, Pearson correlations between the relative abundances of taxa and the MCMV titers were calculated. Analysis were performed using the Rhea script pipeline [57] for the software R.

RNA Extraction and Quantitative (RT-qPCR). RNA was isolated from small explants of the distal part of the colon using the RNAeasy Fibrous Tissue Kit (Qiagen, Hilden, Germany) following the manufacturer's instructions. To synthesize cDNA, RNA was reverse transcribed using M-MLV Reverse Transcriptase (Promega, Mannheim, Germany) with dNTPs, Oligo-dT mixed with random hexamer primers (Thermo Fisher Scientific). Quantitative PCR was conducted using the SYBR Green PCR Kit (Thermo Fisher Scientific), specific primers (Table 1) and cDNA of the colon biopsies or the genomic DNA of the feces samples. Relative mRNA levels of *Reg3γ* were defined by using the included standard curve

for each individual gene and further normalization to the reference gene ribosomal protein S9 (*Rps9*). The proportion of higher bacterial taxa in the feces were calculated using the Cts of *Bacteroidetes* and *Firmicutes* referred to the total *16S* DNA within each sample as described by Yang *et al*. 2015 [54].

Histopathological analysis. Full-length colons were stored in 4% (w/v) paraformaldehyde and embedded in paraffin. Sections (4 μm) were prepared from paraffin-embedded blocks, stained with hematoxylin and eosin (H&E), and evaluated in a blinded manner according to standard techniques as described previously [58]. Crypt necrosis is defined as a flattening of the crypt epithelial cells and presence of dead cells/cellular debris in the crypt lumina. For crypt hyperplasia, the mean length value of 30 crypts per colon was calculated. Caspase-3 staining was performed as described earlier [59]. Images were dearrayed using Fiji ImageJ (Version 1.52i) and the color deconvolution plugin, resulting in individual channels for hematoxylin (H); nucleus and DNA) and 3,3′-Diaminobenzidine (DAB; caspase-3). Specific threshold was set for DNA and caspase-3 and images were pseudo-colored in blue (DNA) and red (caspase-3), respectively, after which images were merged. Five mice per group and three image sections per mouse were analyzed for caspase-3 positive epithelial cells. Image sections were selected and quantified in a blinded manner.

For GFP-staining, sections were deparaffinized and antigen was retrieved using 1 mM Tris solution (pH 9.0) for 30 min at 95 °C. All staining reactions were performed by automated staining using a BOND RX autostainer (Leica Biosystems). Sections were stained with a rabbit anti-GFP primary antibody (Novus Biologicals #NB600-308) diluted 1:1000 in Ventana Antibody Diluent with Casein (Roche #6440002001). A detection kit from Leica Biosystems was used (BOND Polymer Refine Detection; #DS9800) that includes a polymeric horseradish peroxidase (HRP)-linker antibody conjugate system for the detection of tissue-bound mouse and rabbit IgG; 3,3-diaminobenzidine (DAB) as a brown chromogen (from

Leica Biosystems). Finally, the samples were counterstained with hematoxylin and mounted with Pertex (Biosystems). Slides were scanned using a Pannoramic 250 digital scanner (3DHISTECH).

Human tissue sections were fixed in 4% formaldehyde and embedded in paraffin. All staining reactions were performed by automated staining using a BOND III autostainer (Leica Biosystems, Wetzlar, Germany). For immunohistochemistry, sections were deparaffinized and antigen was retrieved using 1 mM Tris solution (pH 9.0) for 30 min at 95°C. Sections were stained with mouse anti human CMV (Dako, Agilent technologies, Glostrup, Denmark) primary antibody. Specific binding of primary antibodies was visualized using a polymer-based visualizing system with horseradish peroxidase as the enzyme and 3,3-diaminobenzidine (DAB) as a brown chromogen, (Bond™ Polymer Refine DAB Detection from Leica Biosystems). Finally, the samples were counterstained with haematoxylin and mounted with Eukitt (O. Kindler GmbH, Freiburg, Germany) before scanning. After staining, slides were scanned using a Pannoramic 250 digital scanner (3DHISTECH).

Colon explant culture and cytokine detection. A small explant (15-25 µg) from the distal part of the colon was cultured for 6 h in IMDM complete medium (IMDM containing GlutaMax^{TM} -I, 25 mM HEPES, 10% FCS, 100 µg/ml streptomycin, 100 U/ml penicillin, 25 µM β-mercaptoethanol). Cytokine levels in the supernatants were measured by Luminex technology (R&D Systems, Wiesbaden, Germany) on a Luminex 200 instrument using the Luminex IS software (Luminex Corporation, MV's-Hertogenbosch, Netherlands). Cytokine concentration was normalized to the respective weight of the colon biopsies.

FITC-dextran intestinal permeability assay. Non-infected and MCMV-infected mice were orally gavaged with 150 µl of 100 mg/ml 4 kDa FITC-dextran-labeled dextran beads (Sigma-Aldrich/Merck, Darmstadt, Germany) in PBS 4 hours prior to sacrifice. Blood was collected from the heart and allowed to clot completely for 1 h at room temperature. Then blood

samples were centrifuged at 4500 g for 15 min to obtain the serum. Serum was measured in 1:5 and 1:10 (v/v) dilutions with PBS. FITC-derived fluorescence was quantified in the serum using a microplate multireader (Mithras LB 943). Concentrations were determined using a standard curve generated by serial dilution of FITC-dextran.

Crypt isolation from murine intestine. Small intestinal samples were rinsed with ice-cold PBS and cut into 5-mm pieces. Tissue segments were washed multiple times with cold PBS and incubated in 5 mM EDTA-PBS for 30 min gently shaking on ice. To release crypts, tissue pieces were shaken twice vigorously in cold PBS for 30 s. The crypt suspension was passed through a 100-µm cell strainer, pelleted at 300 g for 5 min and washed at 60 g for 3 min to remove single cells. Crypts were plated in 40 µl matrigel (Corning, Tewksbury, MA, USA) and cultured with 500 µl/well murine IntestiCult^{TM} Organoid Growth Medium (OGM, Stemcell Technologies, Cologne, Germany). Medium was changed every 2-3 days. MCMV infection was performed after 7 days of culture.

Crypt isolation from murine colon, enteroid forming efficiency and survival. Colonic crypt isolation was performed as described previously [60]. Briefly, the distal colon was flushed with ice-cold PBS containing antibiotics and minced into 2-mm pieces. Tissue fragments were digested in 10 ml DMEM containing 1% (v/v) FCS, antibiotics, and 500 U/ml collagenase IV. Crypts were released by shaking and pipetting the tissue fragments vigorously. Isolated crypts were passed through a 100-µm cell strainer, pelleted, washed and embedded in matrigel. After polymerization, 500 µl/well of murine IntestiCult^{TM} OGM were added. The enteroid forming efficiency was determined by counting the exact number of crypts after plating and the organoids formed from the crypts after 24 h. For enteroid survival, the amount of intact organoids was determined every second day for one week after crypt isolation.

Crypt isolation from human colon biopsies. Colonic biopsies were washed several times with ice-cold PBS and incubated in 2.5 mM EDTA-PBS at 4 °C for 40 min. Tissue fragments were suspended vigorously in ice-cold PBS with a bovine serum albumin (BSA)-coated 10 ml pipette. This step was repeated three times and the supernatants containing crypts were transferred to a BSA-coated tube. Crypts were pelleted at 1600 rpm for 3 min, plated in matrigel, and cultured with 500 µl/well human IntestiCult™ OGM (Stemcell Technologies). Medium was changed every 2-3 days and organoids were passaged once a week. After the second passage, organoids were used for HCMV infection.

CMV infection of organoids and assessment of organoid morphology. Organoids were collected in 500 µl/well cell recovery solution (Corning) and incubated for 30 min on ice to depolymerize the matrigel. The organoids were pelleted at 300 g for 3 min and washed with DMEM twice. Afterwards, organoids were resuspended in virus standard buffer (VSB) (Mock), MCMV-GFP, MCMV-m*Cherry,* UV-irradiated MCMV-GFP or the human CMV strain TB40EΔgpt EGFP diluted in DMEM for different multiplicities of infection (MOI) and incubated for 30 min at 37°C. Thereafter, samples were briefly placed on ice, embedded in matrigel and cultured with IntestiCult™ Organoid Growth Medium. Regarding morphology, organoids were classified into four groups (intact budding, intact not budding, partially intact, and destroyed organoids) and counted by light microscopy at 6 days post-infection.

Microscopy. Fluorescence microscopy was performed on an AxioObserver Z1 widefield microscope using a 20x objective and Axiocam 506 mono camera and on Leica Thunder Imager. Images were taken with Leica THUNDER imager using a 20x and 40x objective (Leica DFC9000 GT). Images were processed using computational large volume clearing method. Confocal laser scanning microscopy (CLSM) was performed with a TCS SP8 AOBS system operated by the LASX software (Leica Microsystems). Images were acquired with HC PL Fluotar 10x/0.3, HC PL APO 20x/0.75 CS2, and HCX PL Apo 63x/1.4 oil objectives.

Imaging conditions: pinhole 1 AU, laser intensity 5%. The spheroid images were all recorded with the same set of parameters.

Statistics. Statistical analyses were performed in R or in GraphPad Prism. All statistical tests were performed with significance and confidence level of 0.05.

Ethics Approval.

Ethical approval for human biopsies was provided by the Medical Faculty of the University of Duisburg-Essen (AZ 21-9864-BO). Animal experiments were performed in accordance to the ethical principles and federal guidelines and approved by the Landesamt für Natur, Umwelt und Verbraucherschutz (LANUV, Germany; AZ 81-02.04.2020.A300, 84-02.04.2014.A390, 84-02.04.2013.A414 and 84-02.04.2016.A441).

Data availability.

16S rRNA gene data are deposited in the NCBI SRA (SRA: BioProject: PRJNA763375). Further data that support the findings of this study are available from the corresponding author upon reasonable request.

Conflict of interest

The authors declare no commercial or financial conflict of interest.

Acknowledgement

We kindly thank Mechthild Hemmler-Roloff for excellent technical assistance. The authors are very grateful for a very generous donation from Alantra, based on which the Leica THUNDER Imager was purchased. We thank also the Imaging Center Campus Essen (ICCE), Center of Medical Biotechnology (ZMB), and University of Duisburg-Essen for access to the confocal laser scanning microscopes. We thank the Translational Research Unit (TRU) of the Institute of Pathology of the University of Bern for their excellent technical support. This work was supported by DFG (grants GRK1949, GRK 2098, WE4472/8-1, TR1208/1-1, and TR1208/2-1), Kulturstiftung Essen (grants 106-22078, 106-21590);

Volkswagenstiftung (grant Az. 99 078), and Stiftung Universitätsmedizin Essen (grant 2020 4699 116).

Author contributions.

VTKLT, FB, KW, KRP, MD, BK, and VS performed the experiments and analyzed the data. JFE conceived and conducted the experiments, analyzed the results, and wrote the manuscript. AMW, VTKLT, and MT designed and supervised the study, and wrote the manuscript. EL assisted in the microbiome analysis. PK, AA, AM, and RK performed histological analysis. AM, PK, and CML provided human samples and data. All authors contributed to the article and approved the submitted version.

References

1. Rafailidis PI, Mourtzoukou EG, Varbobitis IC, Falagas ME. Severe cytomegalovirus infection in apparently immunocompetent patients: a systematic review. Virol J. 2008;5:47. Epub 2008/03/29. doi: 10.1186/1743-422X-5-47. PubMed PMID: 18371229; PubMed Central PMCID: PMCPMC2289809.
2. Park JH, Moon HS. Cytomegalovirus colitis in immunocompetent patients. Intest Res. 2018;16(3):504-5. Epub 2018/08/10. doi: 10.5217/ir.2018.16.3.504. PubMed PMID: 30090053; PubMed Central PMCID: PMCPMC6077313 was reported.
3. Klauber E, Briski LE, Khatib R. Cytomegalovirus colitis in the immunocompetent host: an overview. Scand J Infect Dis. 1998;30(6):559-64. Epub 1999/05/04. doi: 10.1080/00365549850161098. PubMed PMID: 10225382.
4. Rezania D, Ouban A, Marcet J, Kelley S, Coppola D. CMV colitis mimicking recurrent inflammatory bowel disease: report of three cases. Am Surg. 2007;73(1):58-61. Epub 2007/01/26. PubMed PMID: 17249458.
5. Karigane D, Takaya S, Seki Y, Mastumoto Y, Onose A, Kosakai A, et al. Cytomegalovirus enteritis in immunocompetent subjects: a case report and review of the literature. J Infect Chemother. 2014;20(5):325-9. Epub 2014/04/23. doi: 10.1016/j.jiac.2013.12.004. PubMed PMID: 24751234.
6. Foster A, Jacobson K. Changing incidence of inflammatory bowel disease: environmental influences and lessons learnt from the South asian population. Front Pediatr. 2013;1:34. Epub 2014/01/09. doi: 10.3389/fped.2013.00034. PubMed PMID: 24400280; PubMed Central PMCID: PMCPMC3864265.
7. Sekirov I, Russell SL, Antunes LC, Finlay BB. Gut microbiota in health and disease. Physiol Rev. 2010;90(3):859-904. Epub 2010/07/29. doi: 10.1152/physrev.00045.2009. PubMed PMID: 20664075.
8. de Souza HS, Fiocchi C. Immunopathogenesis of IBD: current state of the art. Nat Rev Gastroenterol Hepatol. 2016;13(1):13-27. Epub 2015/12/03. doi: 10.1038/nrgastro.2015.186. PubMed PMID: 26627550.
9. Dimitroulia E, Spanakis N, Konstantinidou AE, Legakis NJ, Tsakris A. Frequent detection of cytomegalovirus in the intestine of patients with inflammatory bowel disease. Inflamm Bowel Dis. 2006;12(9):879-84. Epub 2006/09/07. doi: 10.1097/01.mib.0000231576.11678.57. PubMed PMID: 16954807.

10. Criscuoli V, Rizzuto MR, Cottone M. Cytomegalovirus and inflammatory bowel disease: is there a link? World J Gastroenterol. 2006;12(30):4813-8. Epub 2006/08/29. doi: 10.3748/wjg.v12.i30.4813. PubMed PMID: 16937462; PubMed Central PMCID: PMCPMC4087614.
11. Streetz KL, Buhr T, Wedemeyer H, Bleck J, Schedel I, Manns MP, et al. Acute CMV-colitis in a patient with a history of ulcerative colitis. Scand J Gastroenterol. 2003;38(1):119-22. Epub 2003/03/01. PubMed PMID: 12608474.
12. Zheng D, Liwinski T, Elinav E. Interaction between microbiota and immunity in health and disease. Cell Res. 2020;30(6):492-506. Epub 2020/05/21. doi: 10.1038/s41422-020-0332-7. PubMed PMID: 32433595; PubMed Central PMCID: PMCPMC7264227.
13. Rooks MG, Garrett WS. Gut microbiota, metabolites and host immunity. Nat Rev Immunol. 2016;16(6):341-52. Epub 2016/05/28. doi: 10.1038/nri.2016.42. PubMed PMID: 27231050; PubMed Central PMCID: PMCPMC5541232.
14. Dillon SM, Lee EJ, Kotter CV, Austin GL, Dong Z, Hecht DK, et al. An altered intestinal mucosal microbiome in HIV-1 infection is associated with mucosal and systemic immune activation and endotoxemia. Mucosal Immunol. 2014;7(4):983-94. Epub 2014/01/09. doi: 10.1038/mi.2013.116. PubMed PMID: 24399150; PubMed Central PMCID: PMCPMC4062575.
15. Gevers D, Kugathasan S, Denson LA, Vazquez-Baeza Y, Van Treuren W, Ren B, et al. The treatment-naive microbiome in new-onset Crohn's disease. Cell Host Microbe. 2014;15(3):382-92. Epub 2014/03/19. doi: 10.1016/j.chom.2014.02.005. PubMed PMID: 24629344; PubMed Central PMCID: PMCPMC4059512.
16. Zevin AS, McKinnon L, Burgener A, Klatt NR. Microbial translocation and microbiome dysbiosis in HIV-associated immune activation. Curr Opin HIV AIDS. 2016;11(2):182-90. Epub 2015/12/19. doi: 10.1097/COH.0000000000000234. PubMed PMID: 26679414; PubMed Central PMCID: PMCPMC4752849.
17. Santos Rocha C, Hirao LA, Weber MG, Mendez-Lagares G, Chang WLW, Jiang G, et al. Subclinical Cytomegalovirus Infection Is Associated with Altered Host Immunity, Gut Microbiota, and Vaccine Responses. J Virol. 2018;92(13). Epub 2018/04/20. doi: 10.1128/JVI.00167-18. PubMed PMID: 29669841; PubMed Central PMCID: PMCPMC6002712.
18. Frank DN, St Amand AL, Feldman RA, Boedeker EC, Harpaz N, Pace NR. Molecular-phylogenetic characterization of microbial community imbalances in human inflammatory bowel diseases. Proc Natl Acad Sci U S A. 2007;104(34):13780-5. Epub 2007/08/19. doi: 10.1073/pnas.0706625104. PubMed PMID: 17699621; PubMed Central PMCID: PMCPMC1959459.
19. Balint A, Farkas K, Mehi O, Kintses B, Vasarhelyi BM, Ari E, et al. Functional Anatomical Changes in Ulcerative Colitis Patients Determine Their Gut Microbiota Composition and Consequently the Possible Treatment Outcome. Pharmaceuticals (Basel). 2020;13(11). Epub 2020/11/01. doi: 10.3390/ph13110346. PubMed PMID: 33126430; PubMed Central PMCID: PMCPMC7692875.
20. Lucke K, Miehlke S, Jacobs E, Schuppler M. Prevalence of Bacteroides and Prevotella spp. in ulcerative colitis. J Med Microbiol. 2006;55(Pt 5):617-24. Epub 2006/04/06. doi: 10.1099/jmm.0.46198-0. PubMed PMID: 16585651.
21. Le-Trilling VTK, Wohlgemuth K, Ruckborn MU, Jagnjic A, Maassen F, Timmer L, et al. STAT2-Dependent Immune Responses Ensure Host Survival despite the Presence of a Potent Viral Antagonist. J Virol. 2018;92(14). Epub 2018/05/11. doi: 10.1128/JVI.00296-18. PubMed PMID: 29743368; PubMed Central PMCID: PMCPMC6026732.
22. Suzuki T, Yoshinaga N, Tanabe S. Interleukin-6 (IL-6) regulates claudin-2 expression and tight junction permeability in intestinal epithelium. J Biol Chem. 2011;286(36):31263-71. Epub 2011/07/21. doi: 10.1074/jbc.M111.238147. PubMed PMID: 21771795; PubMed Central PMCID: PMCPMC3173073.
23. Bruewer M, Utech M, Ivanov AI, Hopkins AM, Parkos CA, Nusrat A. Interferon-gamma induces internalization of epithelial tight junction proteins via a macropinocytosis-like process.

FASEB J. 2005;19(8):923-33. Epub 2005/06/01. doi: 10.1096/fj.04-3260com. PubMed PMID: 15923402.
24. Rattay S, Trilling M, Megger DA, Sitek B, Meyer HE, Hengel H, et al. The Canonical Immediate Early 3 Gene Product pIE611 of Mouse Cytomegalovirus Is Dispensable for Viral Replication but Mediates Transcriptional and Posttranscriptional Regulation of Viral Gene Products. J Virol. 2015;89(16):8590-8. Epub 2015/06/13. doi: 10.1128/JVI.01234-15. PubMed PMID: 26063418; PubMed Central PMCID: PMCPMC4524224.
25. Clevers H. The intestinal crypt, a prototype stem cell compartment. Cell. 2013;154(2):274-84. Epub 2013/07/23. doi: 10.1016/j.cell.2013.07.004. PubMed PMID: 23870119.
26. Clevers H. Modeling Development and Disease with Organoids. Cell. 2016;165(7):1586-97. Epub 2016/06/18. doi: 10.1016/j.cell.2016.05.082. PubMed PMID: 27315476.
27. Jorgensen I, Rayamajhi M, Miao EA. Programmed cell death as a defence against infection. Nat Rev Immunol. 2017;17(3):151-64. Epub 2017/02/01. doi: 10.1038/nri.2016.147. PubMed PMID: 28138137; PubMed Central PMCID: PMCPMC5328506.
28. Brune W, Andoniou CE. Die Another Day: Inhibition of Cell Death Pathways by Cytomegalovirus. Viruses. 2017;9(9). Epub 2017/09/05. doi: 10.3390/v9090249. PubMed PMID: 28869497; PubMed Central PMCID: PMCPMC5618015.
29. Ljungman P, Boeckh M, Hirsch HH, Josephson F, Lundgren J, Nichols G, et al. Definitions of Cytomegalovirus Infection and Disease in Transplant Patients for Use in Clinical Trials. Clin Infect Dis. 2017;64(1):87-91. Epub 2016/10/30. doi: 10.1093/cid/ciw668. PubMed PMID: 27682069.
30. Kandiel A, Lashner B. Cytomegalovirus colitis complicating inflammatory bowel disease. Am J Gastroenterol. 2006;101(12):2857-65. Epub 2006/10/10. doi: 10.1111/j.1572-0241.2006.00869.x. PubMed PMID: 17026558.
31. Maher MM, Nassar MI. Acute cytomegalovirus infection is a risk factor in refractory and complicated inflammatory bowel disease. Dig Dis Sci. 2009;54(11):2456-62. Epub 2008/12/19. doi: 10.1007/s10620-008-0639-6. PubMed PMID: 19093204.
32. Brizic I, Lisnic B, Brune W, Hengel H, Jonjic S. Cytomegalovirus Infection: Mouse Model. Curr Protoc Immunol. 2018;122(1):e51. Epub 2018/07/26. doi: 10.1002/cpim.51. PubMed PMID: 30044539; PubMed Central PMCID: PMCPMC6347558.
33. Ley RE, Turnbaugh PJ, Klein S, Gordon JI. Microbial ecology: human gut microbes associated with obesity. Nature. 2006;444(7122):1022-3. Epub 2006/12/22. doi: 10.1038/4441022a. PubMed PMID: 17183309.
34. Ni J, Wu GD, Albenberg L, Tomov VT. Gut microbiota and IBD: causation or correlation? Nat Rev Gastroenterol Hepatol. 2017;14(10):573-84. Epub 2017/07/27. doi: 10.1038/nrgastro.2017.88. PubMed PMID: 28743984; PubMed Central PMCID: PMCPMC5880536.
35. Brunson JL, Becker F, Stokes KY. The impact of primary and persistent cytomegalovirus infection on the progression of acute colitis in a murine model. Pathophysiology. 2015;22(1):31-7. Epub 2014/12/17. doi: 10.1016/j.pathophys.2014.11.001. PubMed PMID: 25511533; PubMed Central PMCID: PMCPMC4329059.
36. Matsumura K, Nakase H, Kosugi I, Honzawa Y, Yoshino T, Matsuura M, et al. Establishment of a novel mouse model of ulcerative colitis with concomitant cytomegalovirus infection: in vivo identification of cytomegalovirus persistent infected cells. Inflamm Bowel Dis. 2013;19(9):1951-63. Epub 2013/07/11. doi: 10.1097/MIB.0b013e318293c5bf. PubMed PMID: 23839229.
37. Onyeagocha C, Hossain MS, Kumar A, Jones RM, Roback J, Gewirtz AT. Latent cytomegalovirus infection exacerbates experimental colitis. Am J Pathol. 2009;175(5):2034-42. Epub 2009/10/10. doi: 10.2353/ajpath.2009.090471. PubMed PMID: 19815702; PubMed Central PMCID: PMCPMC2774067.
38. Xuan L, Ren L, Han F, Gong L, Wan Z, Yang S, et al. Cytomegalovirus Infection Exacerbates Experimental Colitis by Promoting IL-23 Production. Inflammation. 2020;43(1):326-35. Epub 2019/11/09. doi: 10.1007/s10753-019-01122-x. PubMed PMID: 31701354.

39. D'Cruz R T, Lau CC, Thamboo TP. Severe ischemic cytomegalovirus proctocolitis with multiple perforation. Arch Virol. 2018;163(7):1927-31. Epub 2018/03/14. doi: 10.1007/s00705-018-3792-z. PubMed PMID: 29532267.
40. Hasegawa T, Aomatsu K, Nakamura M, Aomatsu N, Aomatsu K. Cytomegalovirus colitis followed by ischemic colitis in a non-immunocompromised adult: a case report. World J Gastroenterol. 2015;21(12):3750-4. Epub 2015/04/04. doi: 10.3748/wjg.v21.i12.3750. PubMed PMID: 25834346; PubMed Central PMCID: PMCPMC4375603.
41. Dennis EA, Smythies LE, Grabski R, Li M, Ballestas ME, Shimamura M, et al. Cytomegalovirus promotes intestinal macrophage-mediated mucosal inflammation through induction of Smad7. Mucosal Immunol. 2018;11(6):1694-704. Epub 2018/08/05. doi: 10.1038/s41385-018-0041-4. PubMed PMID: 30076393; PubMed Central PMCID: PMCPMC7405939.
42. Yokoyama Y, Yamakawa T, Hirano T, Kazama T, Hirayama D, Wagatsuma K, et al. Current Diagnostic and Therapeutic Approaches to Cytomegalovirus Infections in Ulcerative Colitis Patients Based on Clinical and Basic Research Data. Int J Mol Sci. 2020;21(7). Epub 2020/04/05. doi: 10.3390/ijms21072438. PubMed PMID: 32244555; PubMed Central PMCID: PMCPMC7177554.
43. Vanlangenakker N, Vanden Berghe T, Krysko DV, Festjens N, Vandenabeele P. Molecular mechanisms and pathophysiology of necrotic cell death. Curr Mol Med. 2008;8(3):207-20. Epub 2008/05/14. doi: 10.2174/156652408784221306. PubMed PMID: 18473820.
44. Maidji E, Somsouk M, Rivera JM, Hunt PW, Stoddart CA. Replication of CMV in the gut of HIV-infected individuals and epithelial barrier dysfunction. PLoS Pathog. 2017;13(2):e1006202. Epub 2017/02/28. doi: 10.1371/journal.ppat.1006202. PubMed PMID: 28241080; PubMed Central PMCID: PMCPMC5328284.
45. Blander JM. On cell death in the intestinal epithelium and its impact on gut homeostasis. Curr Opin Gastroenterol. 2018;34(6):413-9. Epub 2018/09/01. doi: 10.1097/MOG.0000000000000481. PubMed PMID: 30169459; PubMed Central PMCID: PMCPMC6462190.
46. el Marjou F, Janssen KP, Chang BH, Li M, Hindie V, Chan L, et al. Tissue-specific and inducible Cre-mediated recombination in the gut epithelium. Genesis. 2004;39(3):186-93. Epub 2004/07/30. doi: 10.1002/gene.20042. PubMed PMID: 15282745.
47. Le-Trilling VT, Trilling M. Mouse newborn cells allow highly productive mouse cytomegalovirus replication, constituting a novel convenient primary cell culture system. PLoS One. 2017;12(3):e0174695. Epub 2017/03/25. doi: 10.1371/journal.pone.0174695. PubMed PMID: 28339479; PubMed Central PMCID: PMCPMC5365124.
48. Vidal K, Grosjean I, evillard JP, Gespach C, Kaiserlian D. Immortalization of mouse intestinal epithelial cells by the SV40-large T gene. Phenotypic and immune characterization of the MODE-K cell line. J Immunol Methods. 1993;166(1):63-73. Epub 1993/11/05. doi: 10.1016/0022-1759(93)90329-6. PubMed PMID: 7693823.
49. Jordan S, Krause J, Prager A, Mitrovic M, Jonjic S, Koszinowski UH, et al. Virus progeny of murine cytomegalovirus bacterial artificial chromosome pSM3fr show reduced growth in salivary Glands due to a fixed mutation of MCK-2. J Virol. 2011;85(19):10346-53. Epub 2011/08/05. doi: 10.1128/JVI.00545-11. PubMed PMID: 21813614; PubMed Central PMCID: PMCPMC3196435.
50. Henry SC, Schmader K, Brown TT, Miller SE, Howell DN, Daley GG, et al. Enhanced green fluorescent protein as a marker for localizing murine cytomegalovirus in acute and latent infection. J Virol Methods. 2000;89(1-2):61-73. Epub 2000/09/21. doi: 10.1016/s0166-0934(00)00202-0. PubMed PMID: 10996640.
51. Trilling M, Le VT, Rashidi-Alavijeh J, Katschinski B, Scheller J, Rose-John S, et al. "Activated" STAT proteins: a paradoxical consequence of inhibited JAK-STAT signaling in cytomegalovirus-infected cells. J Immunol. 2014;192(1):447-58. Epub 2013/12/10. doi: 10.4049/jimmunol.1203516. PubMed PMID: 24319264.

52. Zimmermann A, Hauka S, Maywald M, Le VTK, Schmidt SK, Daubener W, et al. Checks and balances between human cytomegalovirus replication and indoleamine-2,3-dioxygenase. J Gen Virol. 2014;95(Pt 3):659-70. Epub 2013/12/18. doi: 10.1099/vir.0.061994-0. PubMed PMID: 24337170.
53. Le-Trilling VTK, Becker T, Nachshon A, Stern-Ginossar N, Scholer L, Voigt S, et al. The Human Cytomegalovirus pUL145 Isoforms Act as Viral DDB1-Cullin-Associated Factors to Instruct Host Protein Degradation to Impede Innate Immunity. Cell Rep. 2020;30(7):2248-60 e5. Epub 2020/02/23. doi: 10.1016/j.celrep.2020.01.070. PubMed PMID: 32075763.
54. Yang YW, Chen MK, Yang BY, Huang XJ, Zhang XR, He LQ, et al. Use of 16S rRNA Gene-Targeted Group-Specific Primers for Real-Time PCR Analysis of Predominant Bacteria in Mouse Feces. Appl Environ Microbiol. 2015;81(19):6749-56. Epub 2015/07/19. doi: 10.1128/AEM.01906-15. PubMed PMID: 26187967; PubMed Central PMCID: PMCPMC4561689.
55. Lagkouvardos I, Joseph D, Kapfhammer M, Giritli S, Horn M, Haller D, et al. IMNGS: A comprehensive open resource of processed 16S rRNA microbial profiles for ecology and diversity studies. Sci Rep. 2016;6:33721. Epub 2016/09/24. doi: 10.1038/srep33721. PubMed PMID: 27659943; PubMed Central PMCID: PMCPMC5034312.
56. Lagkouvardos I, Pukall R, Abt B, Foesel BU, Meier-Kolthoff JP, Kumar N, et al. The Mouse Intestinal Bacterial Collection (miBC) provides host-specific insight into cultured diversity and functional potential of the gut microbiota. Nat Microbiol. 2016;1(10):16131. Epub 2016/09/28. doi: 10.1038/nmicrobiol.2016.131. PubMed PMID: 27670113.
57. Lagkouvardos I, Fischer S, Kumar N, Clavel T. Rhea: a transparent and modular R pipeline for microbial profiling based on 16S rRNA gene amplicons. PeerJ. 2017;5:e2836. Epub 2017/01/18. doi: 10.7717/peerj.2836. PubMed PMID: 28097056; PubMed Central PMCID: PMCPMC5234437.
58. Klopfleisch R. Multiparametric and semiquantitative scoring systems for the evaluation of mouse model histopathology--a systematic review. BMC Vet Res. 2013;9:123. Epub 2013/06/27. doi: 10.1186/1746-6148-9-123. PubMed PMID: 23800279; PubMed Central PMCID: PMCPMC3693904.
59. Mabrok HB, Klopfleisch R, Ghanem KZ, Clavel T, Blaut M, Loh G. Lignan transformation by gut bacteria lowers tumor burden in a gnotobiotic rat model of breast cancer. Carcinogenesis. 2012;33(1):203-8. Epub 2011/11/15. doi: 10.1093/carcin/bgr256. PubMed PMID: 22080573.
60. Martin ML, Adileh M, Hsu KS, Hua G, Lee SG, Li C, et al. Organoids Reveal That Inherent Radiosensitivity of Small and Large Intestinal Stem Cells Determines Organ Sensitivity. Cancer Res. 2020;80(5):1219-27. Epub 2019/11/07. doi: 10.1158/0008-5472.CAN-19-0312. PubMed PMID: 31690670; PubMed Central PMCID: PMCPMC7056505.

Table 1 Primer sequences

gene	Forward primer (5'-3')	Reverse primer (3'-5')
Reg3γ	GGCTCCATGACCCGACACT	TAGGCCTTGAATTTGCAGACATAG
Rps9	CTGGACGAGGGCAAGATGAAGC	TGACGTTGGCGGATGAGCACA

target group	Forward primer (5'-3')	Reverse primer (3'-5')
Bacteroidetes	GTTTAATTCGATGATACGCGAG	TTAASCCGACACCTCACGG
Firmicutes	GGAGYATGTGGTTTAATTCGAAGCA	AGCTGACGACAACCATGCAC
16S DNA	AAACTCAAAKGAATTGACGG	CTCACRRCACGAGCTGAC

Figure legends

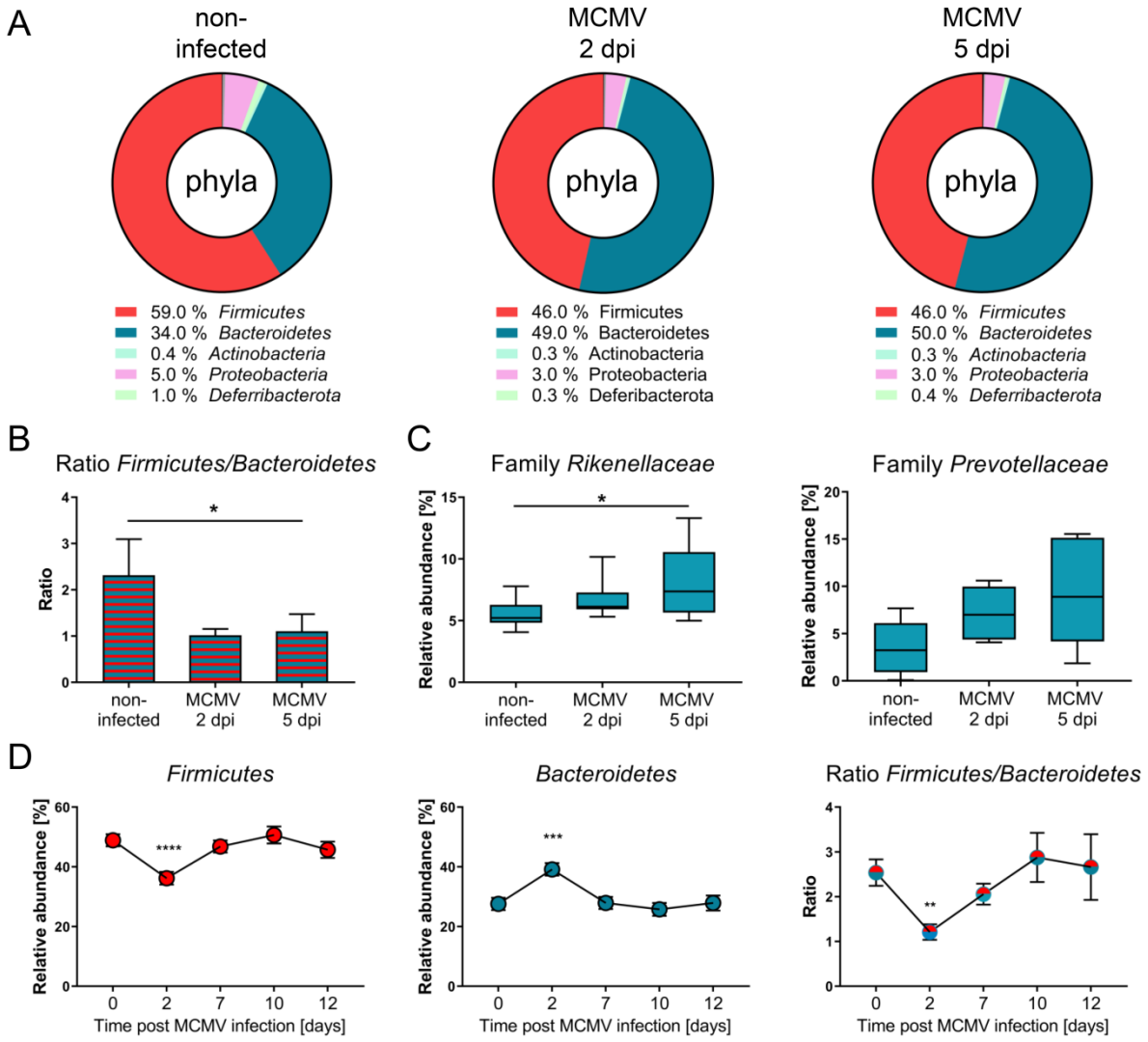

Fig. 1 Acute MCMV infection alters the microbial composition. BALB/c mice were infected (i.p.) with MCMV, and feces samples were taken before infection and at indicated time points post-infection. (A) DNA was extracted and V3-V4 regions of the 16S rRNA gene were sequenced. OTU-based profiles were analyzed using Rhea Script for R. Data were examined regarding relative abundances of the occurring bacterial phyla. (B) Ratio abundance of *Firmicutes* to *Bacteroidetes.* (C) Relative abundance of *Rikenellaceae* and *Prevotellaceae* families. Results (A-C) are from one experiment (n = 6/ group). (D) DNA was extracted and a quantitative PCR was performed for the phyla *Firmicutes* and *Bacteroidetes*. Relative abundance of *Firmicutes* and *Bacteroidetes* in the feces of non-infected and 2 to 12 days infected animals (n = 4/ time point) and ratio abundance of *Firmicutes* to *Bacteroidetes*. Data are shown as mean ± SEM. Statistical analyses were performed

using Friedman test followed by uncorrected Dunn's multiple comparisons test or Student's t-test. *$p < 0.05$

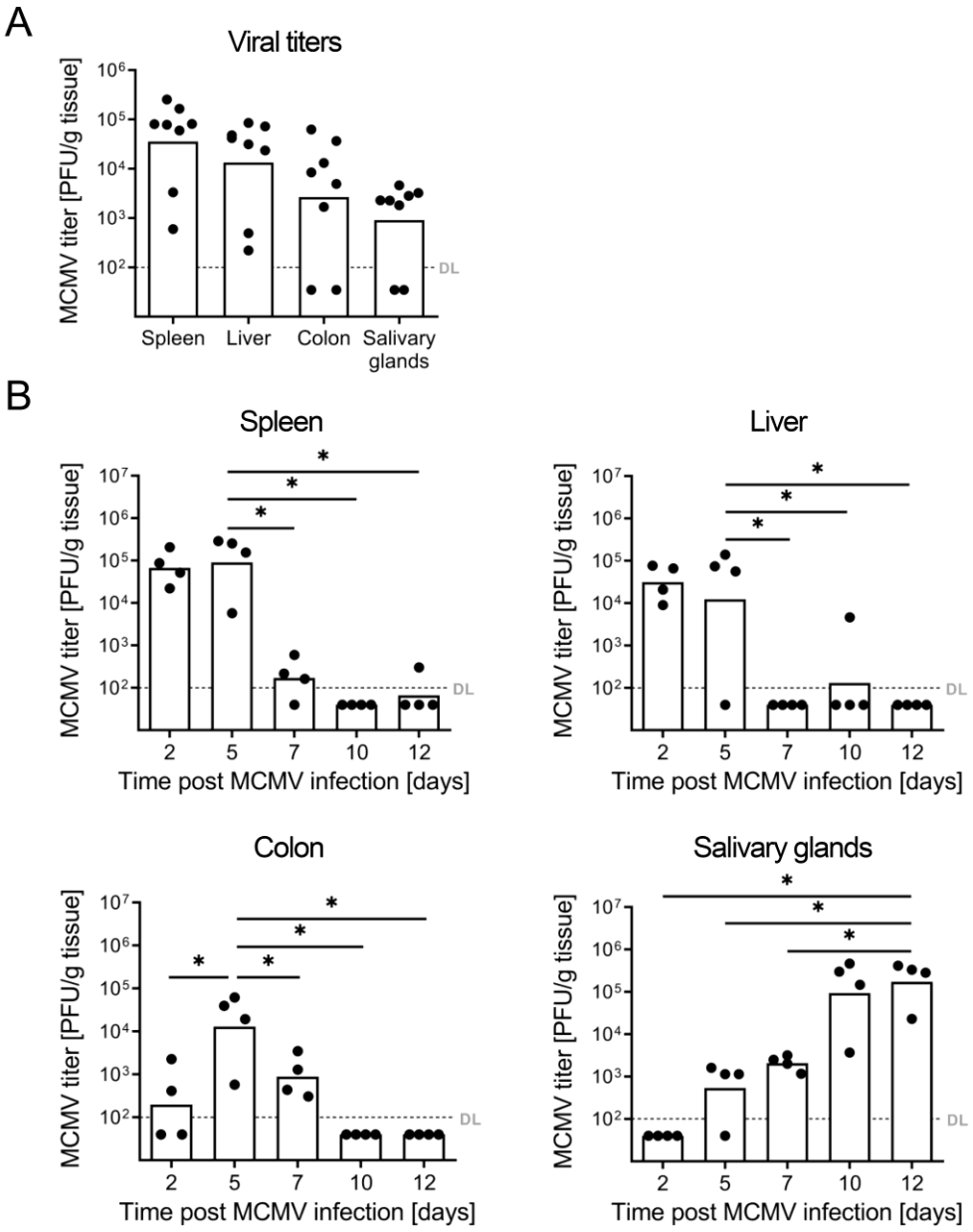

Fig. 2 MCMV replication in the colon. BALB/c mice were infected (i.p.) with MCMV. (A) Viral loads in indicated organs at day 5 post-infection. Data are pooled from two independent experiments (n = 4/ experiment). (B) Viral loads in the spleen, liver, colon, and salivary glands at indicated time points post-infection. Results are from one experiment with n = 4. All titrations were done in quadruplicate. Bars depict the geometric mean, dots show titers of individual mice. DL, detection

limit. One-way ANOVA followed by Tukey's multiple comparison test was used for statistical analysis. *p < 0.05

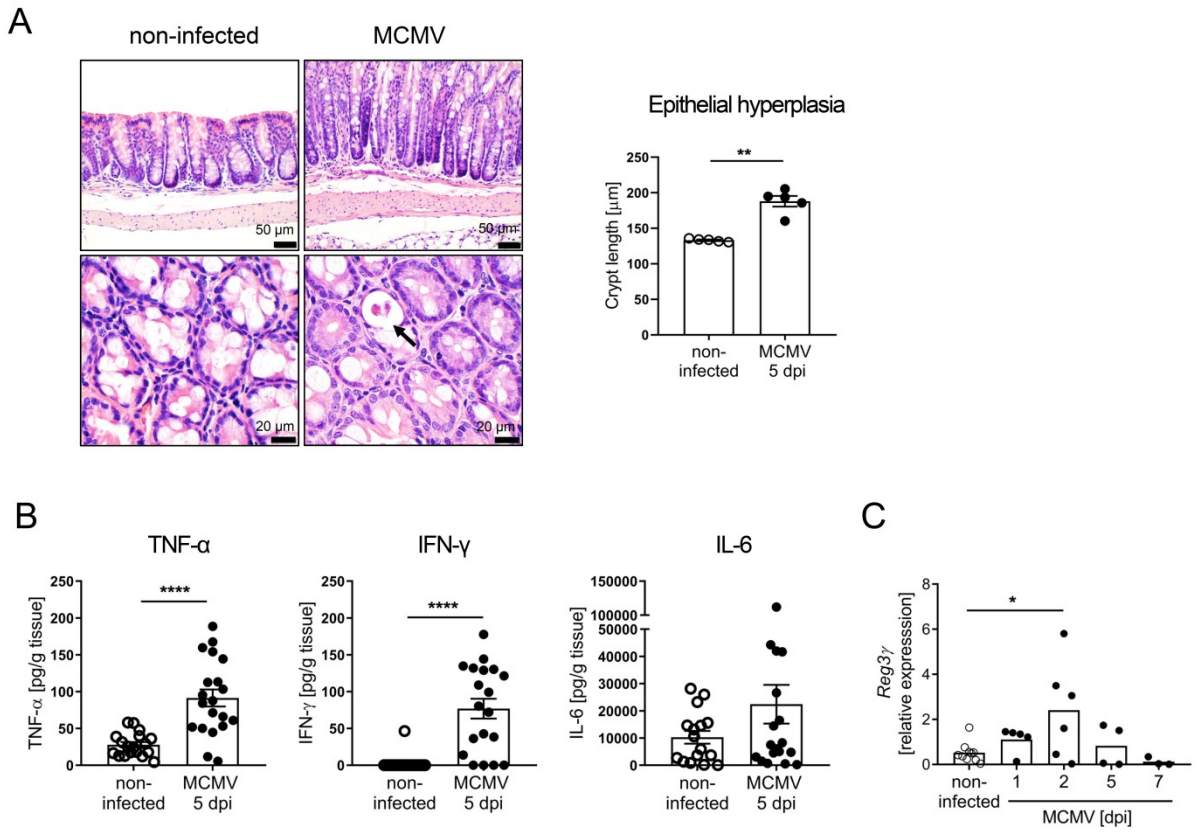

Fig. 3 MCMV replication in the colon is associated with mild colonic inflammation. BALB/c mice were infected with MCMV (i.p.). (A) Representative pictures of H&E-stained colon sections of non-infected mice and mice after 5 days of infection (n = 4/ group). Longitudinal (scale bar 50 µm) and transverse sections (scale bar 20 µm) of colonic crypts are shown. Arrow indicates crypt necrosis. For assessment of epithelial hyperplasia, crypt lengths were measured. (B) Secretion of TNF-α, IFNγ, and IL-6 from *in vitro* cultured colon explants was determined by Luminex technology. Results are from four independent experiments (n = 3-5/group). Data are shown as mean ± SEM. Statistical analyses were performed using Mann-Whitney U test or Student's t-test. *p < 0.05. (C) *Reg3γ* expression normalized to the ribosomal protein S9 gene (*Rps9*) in colon tissue biopsies. Results are from two experiments with n = 3-5. Bars depict the geometric mean, dots show titers of individual mice. One-way ANOVA followed by Tukey's multiple comparison test was used for statistical analysis. *p < 0.05

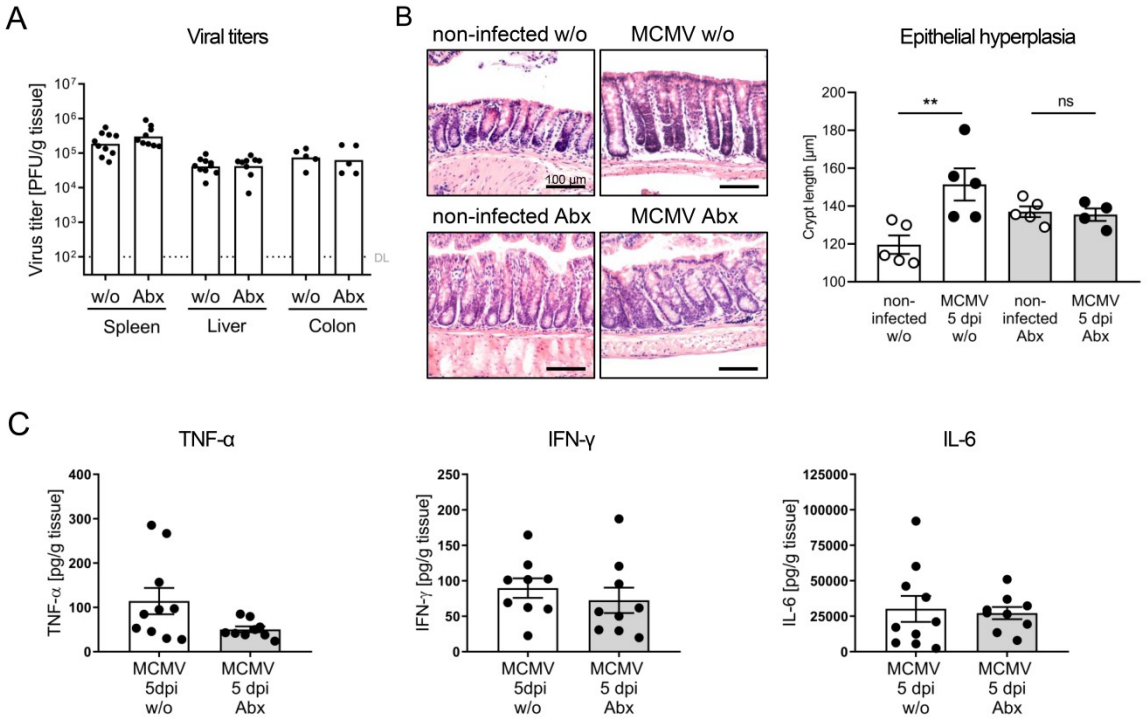

Fig. 4. MCMV infection in absence of microbiota. BALB/c mice were infected (i.p.) with MCMV. (A) Viral loads in spleen, liver, and colon at 5 days post-infection of antibiotic treated and untreated mice. Results are from two experiments with n = 5. All titrations were done in quadruplicate. Bars depict the geometric mean, dots show titers of individual mice. DL, detection limit. (B) Representative pictures (scale bars 50 µm) of H&E-stained colon sections of non-infected mice and mice after 5 days of infection, with and without antibiotic treatment (n = 4-5/ group). For epithelial hyperplasia crypt lengths were measured. One-way ANOVA followed by Tukey's multiple comparison test was used for statistical analysis. $^{**}p < 0.01$ (C) Secretion of TNF-α, IFN-γ, and IL-6 from *in vitro* cultured colon explants was determined by Luminex technology. Results are from two independent experiments (n = 4-5/group). Data are shown as mean ± SEM. Statistical analyses were performed using Mann-Whitney U test, Student's t-test or Student's t-test with Welch's correction. $^{*}p < 0.05$

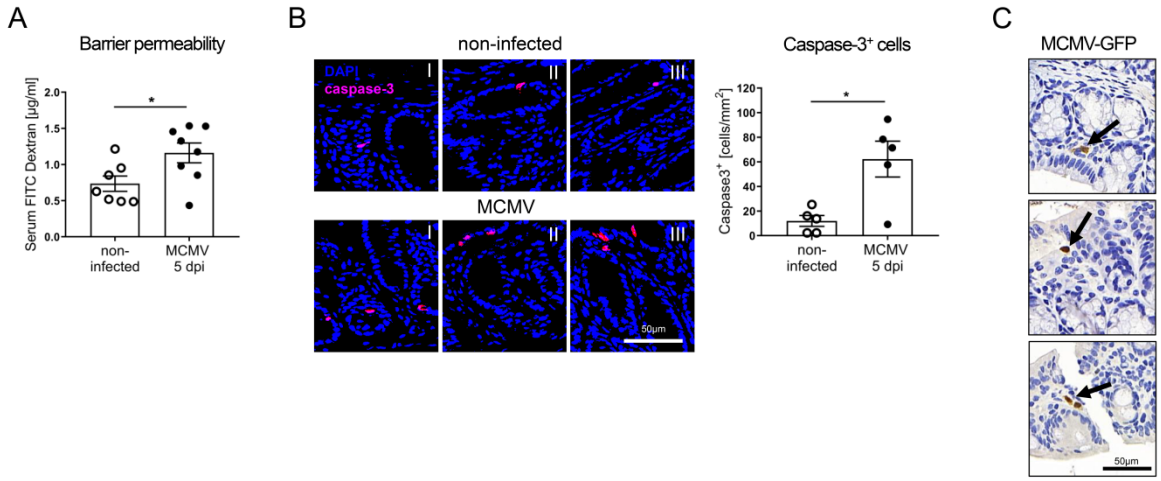

Fig. 5 MCMV replication in the colon reduces the intestinal barrier. BALB/c mice were infected with MCMV (i.p.). (A) At day 5 post-infection, each group of mice (n = 7) received FITC-dextran beads by oral gavage. Serum FITC-dextran concentrations were measured 4 hours after gavage. Data were pooled from two independent experiments. (B) Representative images of immunohistochemistry (IHC) staining on colonic tissue sections of MCMV-infected and non-infected mice (n = 4/ group). IHC was performed using hematoxylin (nucleus and DNA) and DAB (caspase-3). Images were dearrayed via color deconvolution, pseudocolored for nucleus/DNA (blue) and caspase-3 (red), and merged, resulting in caspase-3-positive cells (purple). Scale bar 50µm. (C) Representative images of immunohistochemistry (IHC) staining on horizontally cut colonic tissue sections of MCMV-GFP infected mice (n = 5). IHC was performed using hematoxylin (nucleus and DNA) and DAB (GFP). Arrows indicate DAB stained MCMV infected epithelial cells in crypt cuffs (circular structures). Scale bar 50µm. Data are shown as mean ± SEM. Statistical analysis was performed using Student's t-test or Student's t-test with Welch's correction. *$p < 0.05$

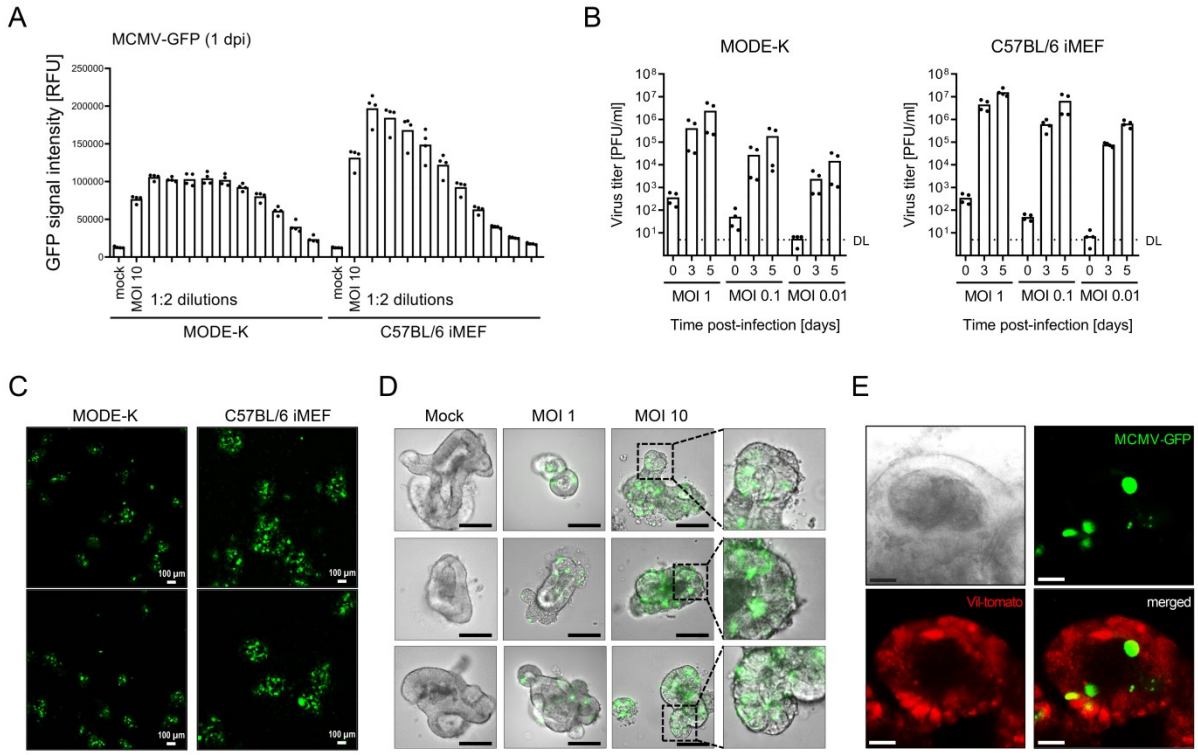

Fig. 6 Intestinal epithelial cells are permissive for cytomegalovirus infection. (A) MODE-K cells and iMEF cells were infected *in vitro* with MCMV-GFP at indicated MOIs (n = 4). Infection efficiency is shown as relative GFP signal intensity. (B) MODE-K cells and iMEF cells were infected with MCMV-GFP at indicated MOIs. At 0, 3, and 5 days post-infection, supernatant was frozen for virus titer determination by standard plaque titration. (C) MODE-K cells and iMEF cells were infected with MCMV-GFP (MOI 0.01). At 3 days post-infection, plaque formation was visualized by image acquisition of GFP-positive cells. (D) Representative images of MCMV-GFP infected intestinal organoids at 1 day post-infection. Scale 100 µm. (E) Differentiated organoids from ROSA26/LSL-tdTom x Villin-Cre (Vil-tomato), which express the tdTomato red fluorescent protein in intestinal epithelial cells, were generated. Organoids (7 days of culture) were infected with MCMV-GFP at an MOI of 10. At day 3 post-infection, immunofluorescence microscopy was performed. Scale bar 20 µm. Representative confocal images of intestinal organoids are shown. Villin-expressing epithelial cells are depicted in red. MCMV-GFP-infected cells show green fluorescence. Representative images of intestinal organoids are shown.

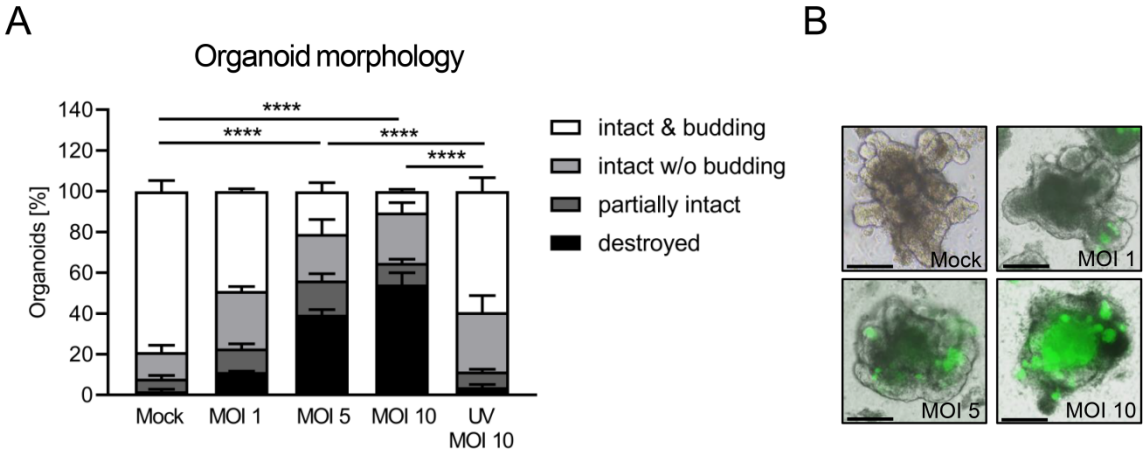

Fig. 7 Cytomegalovirus infection impairs organoid morphology and survival. Intestinal crypts were isolated from BALB/c mice and differentiated to intestinal organoids for 7 days. Organoids were mock treated or infected with increasing MOIs of MCMV-GFP or UV-inactivated MCMV. (A) Organoid morphology was characterized at 6 days post MCMV-GFP infection. One representative experiment out of two is shown (n = 3/ condition). For each sample 70 – 130 organoids were assessed. Data are shown as mean ± SEM. Two-way ANOVA following Tukey's multiple comparisons test for the destroyed group was used for statistical analysis. ****$p < 0.0001$ (B) Representative images of mock treated or MCMV infected organoids at 3 days post-infection are shown. Scale bar 100 µm.

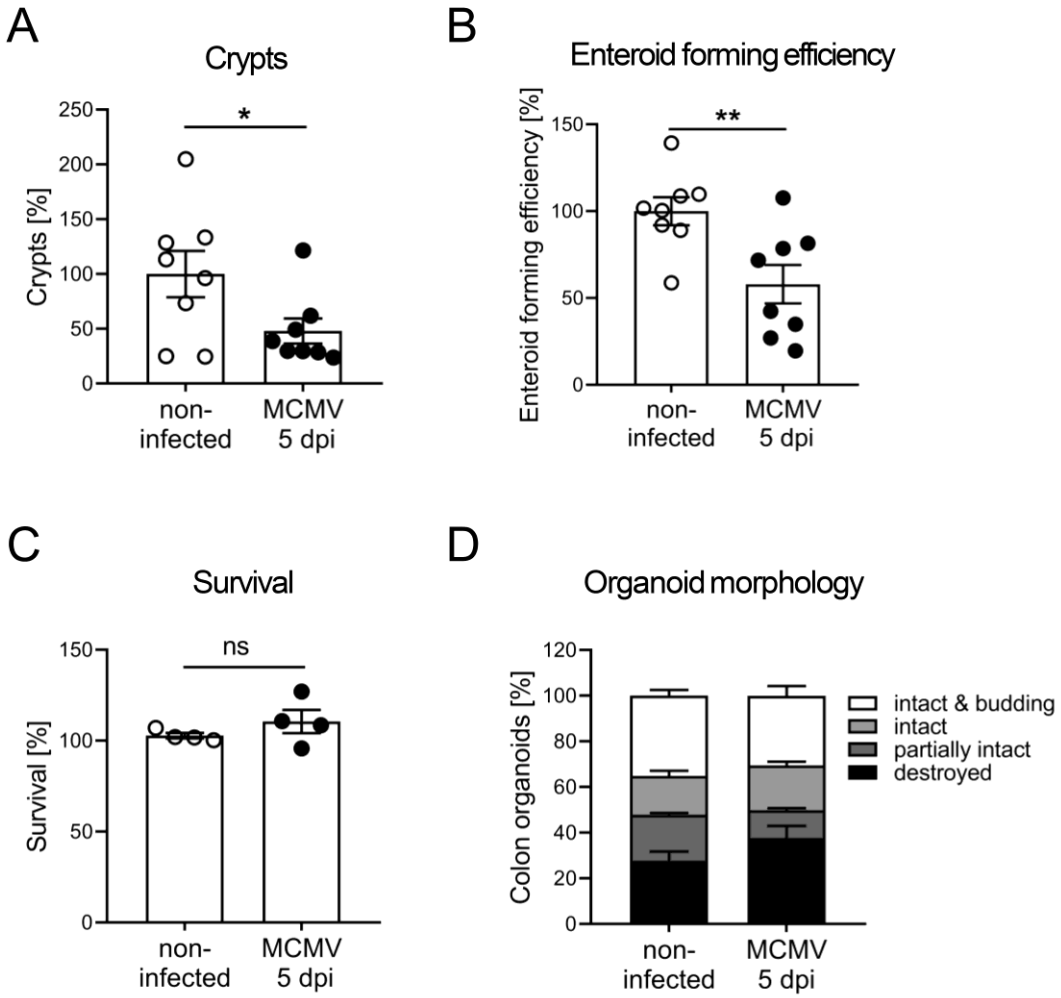

Fig. 8 Cytomegalovirus infection *in vivo* reduces the *ex vivo* enteroid forming efficiency. BALB/c mice were infected with MCMV (i.p.) and at 5 days post-infection colonic crypts were isolated. (A) Relative numbers of isolated colonic crypts (the mean of the absolute number of isolated crypts from non-infected mice was set as 100%, absolute number of isolated crypts was counted in duplicates). (B) Relative enteroid forming efficiency (the mean of the relative enteroid forming efficiency of non-infected mice was set as 100%, enteroid forming efficiency was counted in quadruplicates). In A and B, results from two independent experiments are shown, each dot represents one mouse. (C) Relative organoid survival and the (D) organoid morphology of four mice per group were determined in quadruplicates. Data are shown as mean ± SEM. Statistical analyses were performed using Student's t-test. *$p < 0.05$; **$p < 0.01$

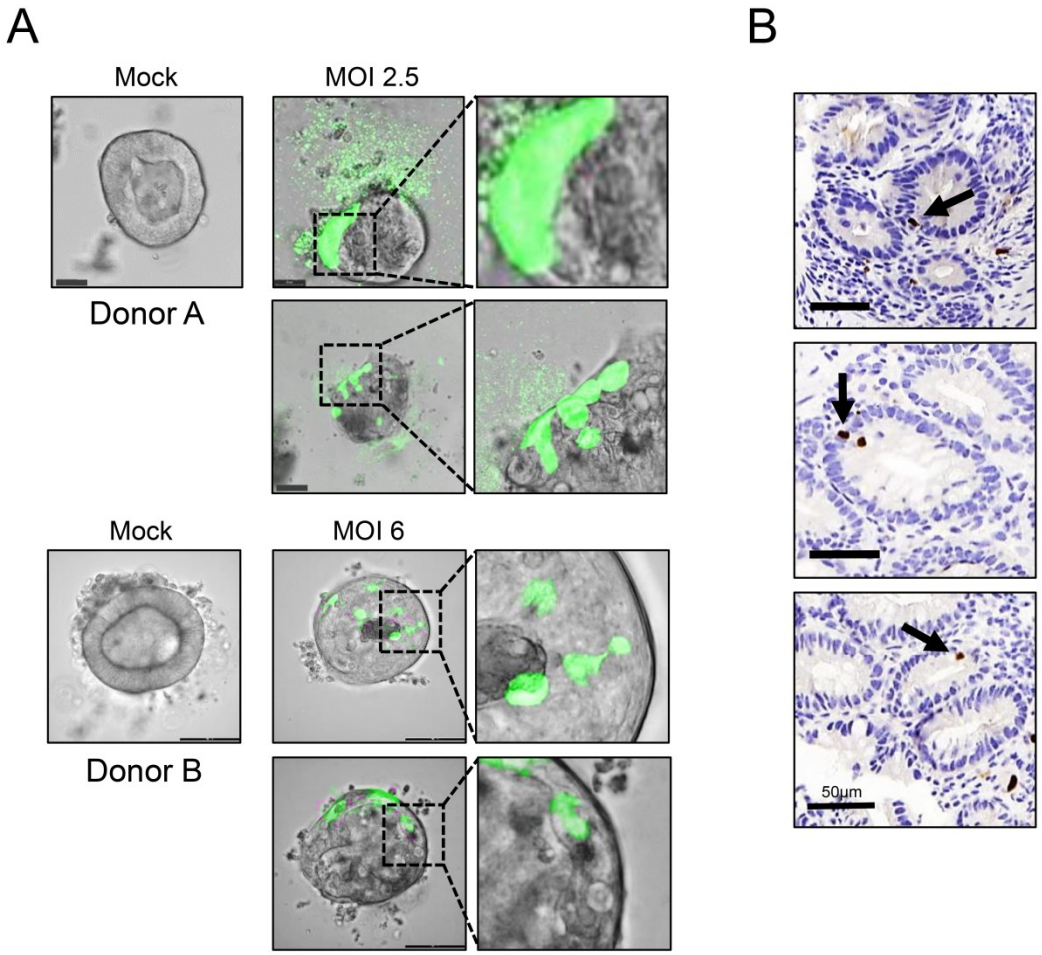

Fig. 9 Human intestinal epithelial cells are permissive for HCMV infection. (A) Differentiated human organoids were generated from colon biopsies of two different healthy donors, mock treated or infected with HCMV-GFP at an MOI of 2.5 (donor A) or MOI of 6 (donor B). At day 3 post-infection, immunofluorescence microscopy was performed. Representative images of intestinal organoids are shown. Scale bar 20 µm for donor A, 100 µm for donor B. (B) Representative images of transverse colonic tissue sections selected from 20 IBD patients with CMV association were stained with mouse anti-human CMV. Arrows indicate DAB stained CMV infected epithelial cells in crypt cuffs (circular structures). Scale bar 50µm.

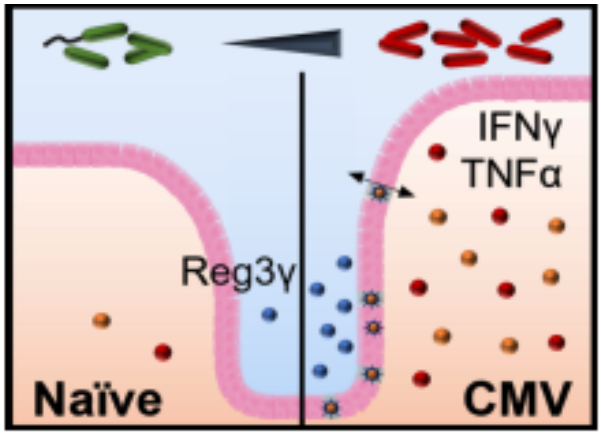

Graphical Abstract_

Acute cytomegalovirus (CMV) infection of immunocompetent mice alters the gut microbiota and